



Contents lists available at ScienceDirect

Bioorganic & Medicinal Chemistry Letters

journal homepage: www.elsevier.com/locate/bmcl

Novel phenylalanine derived diamides as Factor XIa inhibitors



Leon M. Smith II*, Michael J. Orwat, Zilun Hu, Wei Han, Cailan Wang, Karen A. Rossi, Paul J. Gilligan, Kumar B. Pabbisetty, Honey Osuna, James R. Corte, Alan R. Rendina, Joseph M. Luetzgen, Pancras C. Wong, Ranga Narayanan, Timothy W. Harper, Jeffrey M. Bozarth, Earl J. Crain, Anzhi Wei, Vidhyashankar Ramamurthy, Paul E. Morin, Baomin Xin, Joanna Zheng, Dietmar A. Seiffert, Mimi L. Quan, Patrick Y. S. Lam, Ruth R. Wexler, Donald J. P. Pinto

Research and Development, Bristol-Myers Squibb Company, P.O. Box 5400, Princeton, NJ 08543, United States

ARTICLE INFO

Article history:

Received 13 October 2015

Revised 20 November 2015

Accepted 24 November 2015

Available online 26 November 2015

Keywords:

Factor XIa

FXIa

Anticoagulant

Thrombosis

Serine protease

aPTT

ABSTRACT

The synthesis, structural activity relationships (SAR), and selectivity profile of a potent series of phenylalanine diamide FXIa inhibitors will be discussed. Exploration of P1 prime and P2 prime groups led to the discovery of compounds with high FXIa affinity, good potency in our clotting assay (aPTT), and high selectivity against a panel of relevant serine proteases as exemplified by compound **21**. Compound **21** demonstrated good in vivo efficacy ($EC_{50} = 2.8 \mu\text{M}$) in the rabbit electrically induced carotid arterial thrombosis model (ECAT).

© 2015 Elsevier Ltd. All rights reserved.

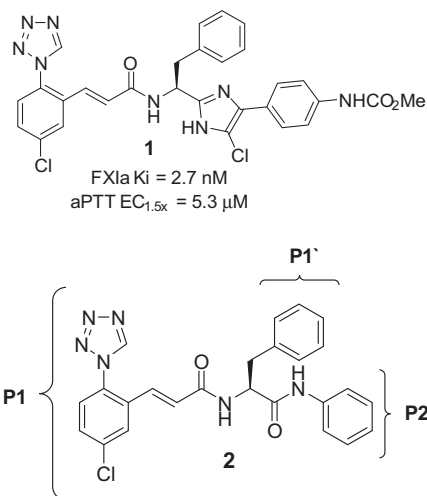
Hemostasis is an adaptive process that maintains blood in a fluid state and preserves vasculature integrity.¹ Disruption of hemostatic balance, if untreated, can lead to thromboembolic complications such as deep vein thrombosis, pulmonary embolism, myocardial infarction, and stroke. Recently, new anticoagulants have been developed that target specific enzymes in the coagulation cascade, such as the thrombin inhibitor, dabigatran (Pradaxa®)² and Factor Xa (FXa) inhibitors, rivaroxaban (Xarelto®),³ apixaban (Eliquis®),⁴ and edoxaban (Savaysa®).⁵ In part, these agents address the limitations seen with the narrow therapeutic index associated with the drug warfarin.⁶ More recently, an intensive effort has been undertaken to identify agents that target FXIa as potential alternative therapies to warfarin prophylaxis.

Factor XI, a serine protease of the intrinsic blood coagulation pathway, is activated to FXIa by thrombin, Factor XIIIa, or FXIa itself. Factor XIa amplifies thrombin generation leading to stable fibrin clot formation. Targeting FXIa inhibition is supported by the observation that human FXI deficiency (hemophilia C) exhibits

a mild bleeding phenotype.⁷ Subjects with high Factor XI plasma levels are at increased thrombosis risk, whereas subjects with severe FXI deficiency have a reduced incidence of ischemic stroke.⁸ Direct, active-site inhibitors of FXIa show robust antithrombotic efficacy with minimum bleeding in rabbit models of thrombosis and hemostasis.^{9a,b} A recent clinical study (VTE prevention after knee replacement surgery) demonstrated that administration of a FXI-directed antisense oligonucleotide (ASO) prevented thrombosis and appeared safe with respect to bleeding.¹⁰ Together, the evidence suggests that FXIa inhibition could block pathologic thrombus formation while preserving normal hemostasis. Recently, our labs disclosed a novel series of phenylimidiazoles^{11a,b} possessing neutral P1 groups including **1** that exhibited good FXIa potency and modest oral exposure in dogs.^{11c} In this report, we describe the utility of these neutral P1 groups in a phenylalanine diamide chemotype **2**. Optimization of the chemotype's P2 prime (P2') and P1 prime (P1') regions will also be discussed.

* Corresponding author. Tel.: +1 609 466 5078; fax: +1 609 818 3450.

E-mail address: leon.smith@bms.com (L.M. Smith).



In designing the phenylalanine diamide chemotype, molecular modeling suggested binding in the FXIa active site would be similar to phenylimidazole analog **1**. It was also postulated that subtle differences could emerge at the P2'.

With this in mind, we began our SAR effort by exploring the P2' group (Table 1). Our initial strategy involved the synthesis of several key analogues possessing optimal P2' moieties previously identified in the phenylimidazole series (compounds **3–5**).^{11,11b} The 4-methoxycarbonylaminophenyl analog **3** exhibited modest FXIa affinity (FXIa $K_i = 40.5$ nM) and greater than 40 μ M activity in the aPTT (clotting) assay^{9c,b} compared to the significantly more potent phenylimidazole compound **1** (FXIa $K_i = 2.7$ nM; aPTT $EC_{1.5x} = 2.7$ μ M). This result supported our prediction that the P2' group SAR would probably deviate between the two series. While aminoindazole **4** and 4-hydroxyquinolin-2(1H)-one **5** analogs performed better than **3**, significant room for further improvements existed. X-ray crystal structure of **1** showed a strong hydrogen bond interaction of the carbamate NH with the carbonyl of His40 and the carbamate carbonyl group with Ile151 interacting through a highly conserved structural water molecule.^{11b} However, modeling of **3** suggested that the methyl carbamate could not efficiently make these same interactions due to the change in torsional angle when compared to the P2' group of **1**. Gratifyingly, 4-benzoic acid analog **6** resulted in a 20-fold increase in FXIa binding affinity (FXIa $K_i = 2$ nM) and a >10-fold improvement in aPTT potency ($EC_{1.5x} = 4.2$ μ M) compared to **3**. The carboxylic acid functionality is within hydrogen bond distance to Tyr143. This modification also led to improved selectivity over plasma kallikrein (PK $K_i = 140$ nM) with a 70:1 selectivity ratio towards FXIa. The 4-phenylacetic acid analog **7** resulted in a >8-fold decrease in FXIa binding affinity (FXIa $K_i = 17$ nM). Meta-substitution as demonstrated by analogs **10** and **11** were relatively less potent.

The X-ray crystal structure of **6** bound in the active site of FXIa at 2.5 Å resolution is depicted in Figure 1.¹² The chlorophenyl tetrazole moiety occupies the S1 pocket with the Cl atom forming an interaction with Tyr228 at the bottom of the S1 pocket, while the tetrazole N-3 atom is optimally oriented within H-bonding distance to the ϵ -amino group of Lys192 (3.1 Å). The tetrazole N-2 nitrogen is near the Lys192 backbone NH (3.3 Å) and the disulfide bridge Cys219–Cys192 (3.1–4.0 Å). The acidic tetrazole CH proton appears to be in close proximity to the carbonyl of Gly216 (3.3 Å). The cinnamide linker carbonyl is positioned nicely within the oxyanion hole by forming key hydrogen bonds with Ser195, Asp194, and Gly193 residues. Overall, the P1 of **6** is similarly

Table 1
Structure–activity relationships of the P2' region

Compound	R	FXIa K_i^a (nM)	PK K_i^a (nM)	aPTT ^b $EC_{1.5x}$ (μ M)
3		40.5	120	>40.0
4		6.4	24	5.75
5		11.2	28	16.5
6		2	140	4.2
7		17	210	>40.0
8		17.5	130	18.8
9		47	170	NT ^c
10		173	350	NT ^c
11		45.6	270	NT ^c

^a K_i values were obtained from purified human enzyme and were averaged from multiple determinations ($n = 2$), as described in Ref. 9.

^b aPTT (activated partial thromboplastin time) in vitro clotting assay was performed in human plasma as described in Ref. 9c.

^c NT = not tested.

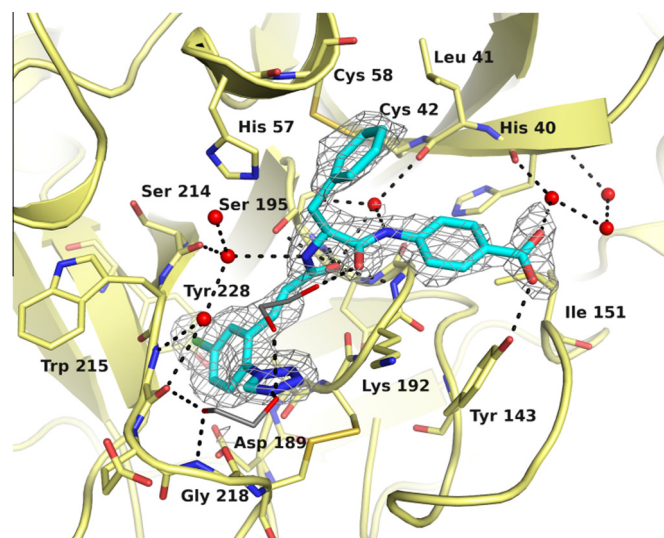


Figure 1. X-ray crystal structure of **6** complexed with FXIa.

oriented to that observed for compound **1**. The benzyl side chain, which occupies the S1' pocket, forms a hydrophobic edge-on contact with the disulfide bridge (Cys42–Cys58). Lastly, the P2' amide

NH makes a water mediated hydrogen bond with Leu41 while the carboxylic acid makes a water mediated hydrogen bond with His40 and a direct hydrogen bond with Tyr143 (2.7 Å) in the enzyme backbone. Overall, the ligand binds to FXIa in a highly efficient manner with each atom on the ligand productively interacting with the enzyme active site residues. The difference in SAR trends between phenylalanine diamides and the phenylimidazole series can be explained by the overlay of co-crystal structures of **6** with **1** as depicted in Figure 2.¹³ The phenyl group of the 4-benzoic acid P2' moiety of **6** does not go as deep into the S2' pocket and is rotated approximately 60° when compared to the 4-methoxycarbonylamino group in **1**. Each motif takes advantage of key hydrogen bond interactions with a complex network of conserved water molecules or via direct interactions with the FXIa enzyme backbone residues.

Next, we decided to expand the SAR of the P2' group by replacing the carboxylic acid moiety in **6** with bioisosteres (Table 2). The C-substituted tetrazole acid bioisostere analog **12** was equipotent while the corresponding N-substituted tetrazole **13** was substantially weaker. Interestingly, **12** led to a decrease in selectivity over plasma kallikrein (16:1). Imidazole **14** and 1*H*-1,2,4-triazole **15** also exhibited satisfactory in vitro results. However, carboxylic acid surrogates 1,2,4-oxadiazol-5(2*H*)-one **16** and 1,3,4-oxadiazol-2(3*H*)-one **17** had good FXIa affinity but were 2–3-fold weaker in the clotting assay which is probably attributable to high protein binding.

We next explored the effect of substitution on the P1' phenyl group (Table 3). It should be noted that introduction of a fluorine in the 2-position of the P1 phenyl **18** resulted in a modest but significant improvement in aPTT potency when compared to **6**. Substitution of the 4-position of the phenyl group with non-polar groups as well as basic groups is well tolerated as exemplified by the FXIa affinities of compounds **19–24**. Propyl analog **19** and biphenyl analog **20** did not offer an advantage when compared to **6** resulting in a >4-fold loss in aPTT potency. However, methylpiperazine urea analog **21** gave improved clotting activity (submicromolar potency) while maintaining good FXIa affinity. Interestingly, inserting fluorine into the P1 phenyl did not enhance aPTT as seen in **18**. Installation of a cyclopropylamide linked hydrophobic P1' analog **23** led to sub-nanomolar FXIa affinity. The boost in affinity may be attributed to the cyclopropyl group having a favorable interaction with the hydrophobic region near Leu41 as depicted in the molecular model of **23** (Fig. 3).

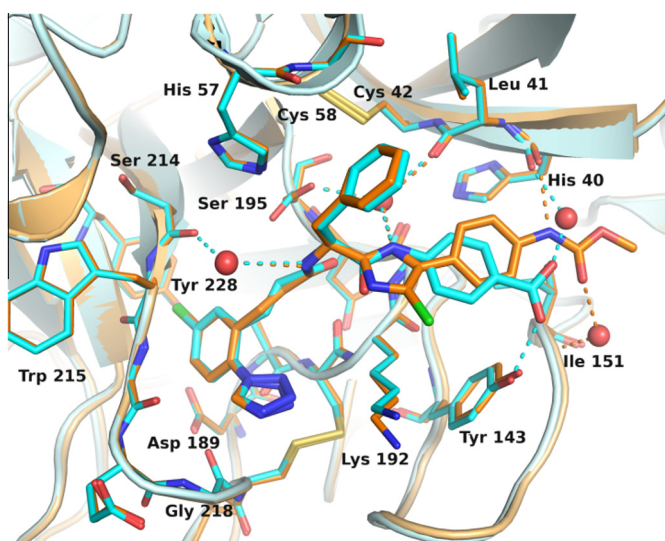
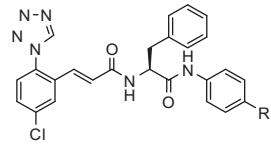


Figure 2. Superposition of crystal structures of diamide **6** (cyan) and phenylimidazole **1** (orange; PDB ID 4Y8X) in active site of FXIa.

Table 2
Carboxylic acid replacement with bioisosteres

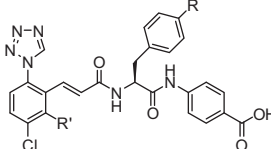


Compound	R	FXIa K_i^a (nM)	PK K_i^a (nM)	aPTT ^b EC _{1.5x} (μM)
6		2	140	4.2
12		1.4	23	4.6
13		43	240	>40.0
14		5.5	150	7.9
15		14	120	8.6
16		2	36	9.6
17		5.8	20	12.7

^a K_i values were obtained from purified human enzyme and were averaged from multiple determinations ($n = 2$), as described in Ref. 9.

^b aPTT (activated partial thromboplastin time) in vitro clotting assay was performed in human plasma as described in Ref. 9c.

Table 3
Structure–activity relationships in the P1 prime region



Compound	R	R'	FXIa/PK K_i^a (nM)	aPTT ^b EC _{1.5x} (μM)
6	H	H	2.0/140	4.2
18	H	F	1.7/46	1.2
19		H	7.1/804	18.5
20		H	11.5/317	38.9
21		H	2.0/59	0.5
22		F	1.8/55	0.7
23^c		F	0.36/7.5	1.5

^a K_i values were obtained from purified human enzyme and were averaged from multiple determinations ($n = 2$), as described in Ref. 9.

^b aPTT (activated partial thromboplastin time) in vitro clotting assay was performed in human plasma as described in Ref. 9c.

^c Diastereomeric mixture.

To further our understanding on how these molecules bound to FXIa, we also evaluated compounds wherein the P1 and P2' groups were reversed (Table 4). To enable the *p*-phenyltetrazole P1 to bind to the S1 region, the reversed diamides required the incorporation of an ethylene linker on the P1 phenyl group. The SAR for compounds **24–27** was the exact opposite for that observed for the previous diamides (Tables 1–3). For example, compounds **24** and **25** were >1000-fold less potent when compared to compounds **6** and **12**. It was interesting to note that the SAR in the reversed diamides series tracked closely to that observed in the phenylimidazole series (e.g., compounds **26** and **27** contain the P2' groups which showed most potency in phenylimidazole series). Superposition of the crystal structures of phenylimidazole **1** and reversed diamide **27** (Fig. 4) reveals the P2' phenyl groups of both chemotypes overlay in a highly efficient manner.^{4a} The primary difference in their binding modes is that P1 linker carbonyl of **27** approaches the oxyanion hole from a higher position but all critical interactions are maintained.

The compounds in Tables 1–3 were prepared according to general synthetic approach outlined in Scheme 1. Boc L-phenylalanine **28** was coupled with P2' anilines **29** in pyridine using phosphoryl oxychloride to give **30** in good yields. This method proved to be particularly useful when electron deficient anilines were employed. Likewise, standard peptide coupling methods can be utilized with electron rich inputs. Intermediates **32a** and **32b** were obtained from commercially available 4-chloro-2-iodoaniline and 2-amino-5-chlorobenzaldehyde using known literature methods.^{13a} The resulting iodo compound **33a** was converted to cinnamate ester **32a** via a Heck cross coupling with ethyl acrylate. Alternatively, a Horner Emmons Wadsworth condensation of benzaldehyde **33b** and methyl diethyl phosphonoacetate provided the corresponding methyl ester **32b**.^{13b} Saponification products **31a** or **31b** and the free amine of **30** were coupled to afford compounds **3–20**.

Advanced intermediates for P2' phenylmethylcarbamate **3** and 4-hydroxyquinolin-2(1*H*)-one **5** compounds in Table 1 were

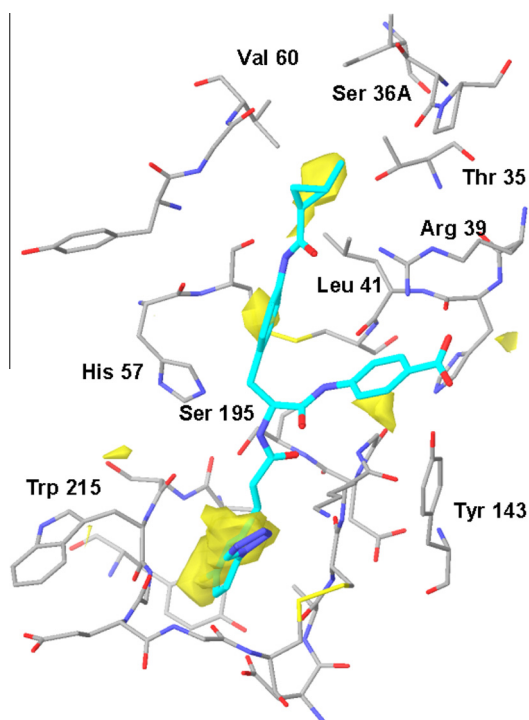
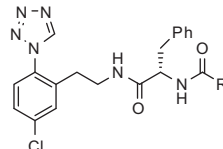
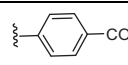
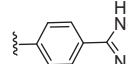
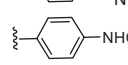
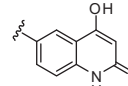


Figure 3. Molecular model of **23** in active site of FXIa.

Table 4
Structure–activity relationship of reversed diamides



Compound	R	FXIa K _i ^a (nM)	PK K _i ^a (nM)	aPTT ^b EC _{1.5x} (μM)
24		2688	>6000	NT ^c
25		1656	>6000	NT ^c
26		3.4	340	4.2
27		1.6	110	1.0

^a K_i values were obtained from purified human enzyme and were averaged from multiple determinations (*n* = 2), as described in Ref. 9.

^b aPTT (activated partial thromboplastin time) in vitro clotting assay was performed in human plasma as described in Ref. 9c.

^c NT = not tested.

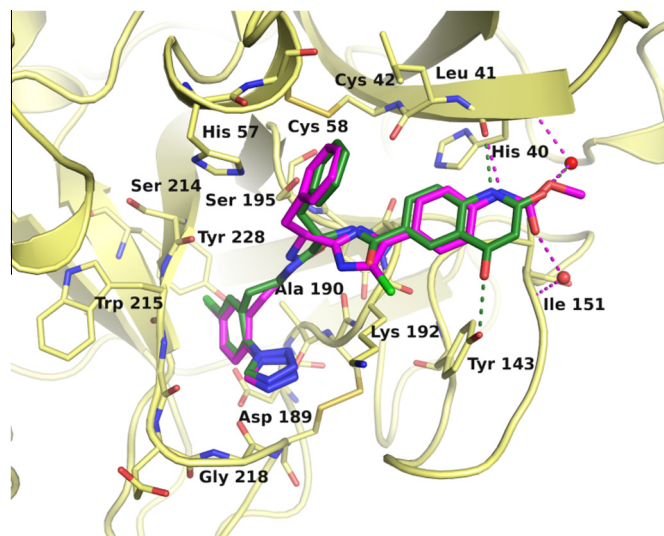
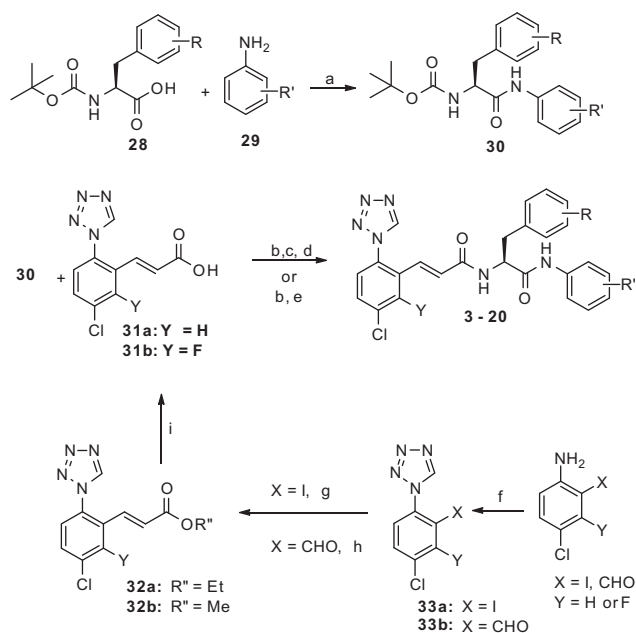


Figure 4. Superposition of crystal structures of reversed diamide **27** (green) and phenylimidazole **1** (magenta) complexed with FXIa.

prepared as shown in Scheme 2 starting from Pd/C catalyzed hydrogenation of **34**. Compound **36** was accessed by treatment of aniline **35** with methyl chloroformate. (*S*)-*tert*-Butyl (1-((4-aminophenyl)amino)-1-oxo-3-phenylpropan-2-yl)carbamate **35** also served as a useful intermediate in the preparation of **38** by coupling with malonic acid mono *tert*-butyl ester followed by cyclization under PPA conditions^{11b} and in situ re-protection of the Boc group in good yields. Aminoindazole compound **4** was prepared from appropriate starting materials utilizing known procedures.¹¹

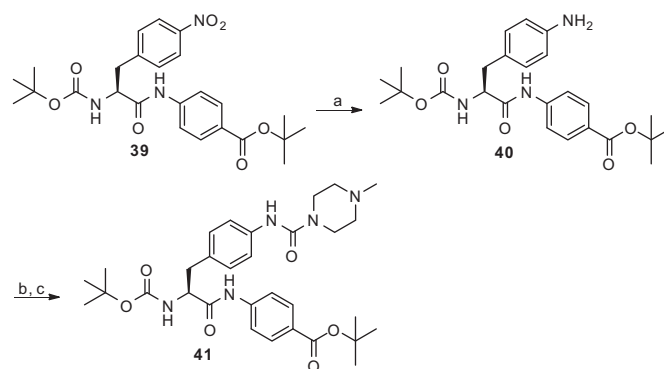
Compound **21** (Table 4) was accessed via nitro reduction of **39** and subsequent urea formation by treatment with triphosgene and *N*-methylpiperazine, respectively, (Scheme 3) and standard attachment of the P1 group. In a similar manner, the cyclopropyl



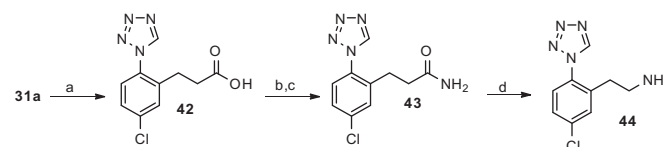
Scheme 1. Reagents and conditions: (a) POCl₃, pyridine, DCM, −15–0 °C, 18–93%; (b) TFA, DCM or HCl, dioxane, 51–95%; (c) 1-hydroxypyrrolidine-2,5-dione, DIC, DMF/THF, 64–100%; (d) DIEA, DMF, 37–73%; (e) EDC, HOBT, DIPEA, DMF, 8–48%; (f) NaN₃, CH(OMe)₃, AcOH, rt, 24 h, 90%; (g) ethyl acrylate, TEA, Pd(OAc)₂, CH₃CN 85 °C, 24 h, 43%; (h) NaH, methyl diethylphosphonoacetate, THF, rt, 24 h, 57%; (i) NaOH, MeOH, water, rt, 94%.

carboxamide **23** was prepared by coupling of **40** with cyclopropyl carboxylic acid under EDC conditions.

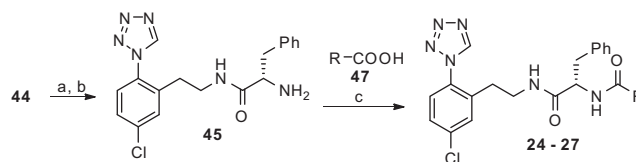
The synthesis of reversed linear diamides in Table 4 is described in Schemes 4 and 5. The double bond of cinnamic acid **31a** was hydrogenated under PtO₂ conditions to give carboxylic acid **42** which was easily converted into primary amide **43** by treatment of the mixed anhydride with ammonia. Compound **43** was subjected to Hofmann degradation to afford primary amine **44** in good yields. The phenyltetrazole phenethyl amine **44** was coupled with Boc-L-phenylalanine **28** followed by TFA deprotection and coupling with appropriate carboxylic acids under EDC/HOBT conditions to give compounds **24–27** (Scheme 5).



Scheme 3. Reagents and conditions: (a) 10% Pd/C, MeOH, H₂, quantitative; (b) trisphosgene, DIPEA; (c) *N*-methylpiperazine, 54%.

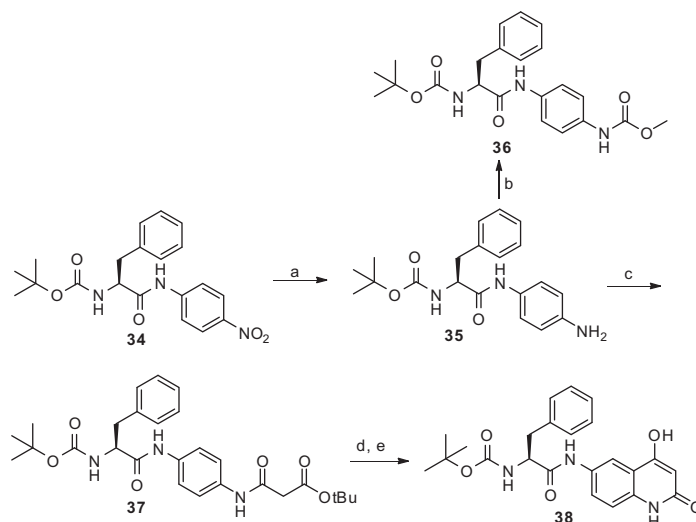


Scheme 4. Reagents and conditions: (a) PtO₂, H₂, MeOH, 83%; (b) ClCO₂Et, Et₃N, THF, −78 °C, (c) NH₃, MeOH; (d) PhI(O₂CCF₃)₂, pyridine, MeCN, H₂O, 95% over three steps.



Scheme 5. Reagents and conditions: (a) Boc-L-phenylalanine **28**, EDC, HOBT, DIPEA, DMF (b) HCl, dioxane, 85% over two steps; (c) EDC, HOBT, DIPEA, DMF, 21–89%.

The pharmacokinetics of representative compounds **6**, **21**, and **27** were evaluated following intravenous administration in dog (Table 5).^{4a} Generally, all compounds exhibited short *t*_{1/2} lives



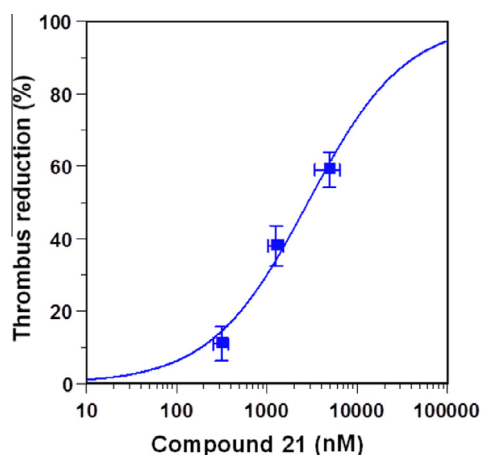
Scheme 2. Reagents and conditions: (a) 10% Pd/C, MeOH, H₂, quantitative; (b) ClCO₂Me, pyridine, DCM, 0 °C, 87–100%; (c) malonic acid mono *tert*-butyl ester, BOP reagent, Et₃N, THF, 92%; (d) PPA, 120 °C; (e) Boc₂O, NaOH, 68% for two steps.

Table 5
Dog PK summary^a

Compound	Cl (mL/min/kg)	Vdss (L/kg)	t _{1/2} (h)	AUC _{tot} (nM * h)
6	16	0.5	0.6	396
21	14	0.7	0.9	314
27	32	1.3	1.0	206

^a Compounds were dosed at 0.4 mg/kg, i.v. in a cassette format.**Table 6**
Enzyme selectivity profiles of compounds **6**, **21**, and **27**

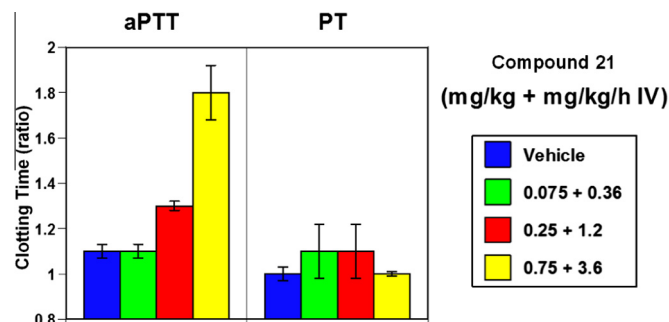
Human enzyme (K _i) ^a	6 (nM)	21 (nM)	27 (nM)
Factor XIa	2.0	2.0	1.6
Factor VIIa	>13,000	>13,000	>13,000
Factor IXa	>73,000	>24,000	>73,000
Factor Xa K _i	5200	>9000	>9000
Factor XIIa	>28,000	>3700	>28,000
Trypsin	>6200	>6200	>6200
Thrombin	>13,000	>13,000	>13,000
Plasma kallikrein	122	59	111
Chymotrypsin	7649	280	1650
Activated protein C	>64,000	>60,000	>64,000
Urokinase	>28,000	>15,000	>28,000
tPA	>46,000	>8,600	>46,000
Tissue kallikrein	>30,000	>30,000	>30,000

^a All K_i values were obtained using human purified enzymes and were averaged from multiple determinations (n = 2).**Figure 5.** Compound **21** in rabbit ECAT model (prevention mode).

(≤1 h). Compounds **6** and **21** exhibited moderate clearance and low volume of distribution while compound **27** had high clearance and volume of distribution.

Table 6 shows the enzyme selectivity comparison of compounds **6**, **21**, and **27**. In general, all three compounds were highly selective over a panel of relevant serine proteases (>1000-fold) including good selectivity over plasma kallikrein (>60-fold). Compound **21** showed less selectivity over chymotrypsin than observed with the other two compounds. The compounds exhibited differentiated human liver stability profiles with **6** and **21** (t_{1/2} = >120 min) being significantly more stable than **27** (t_{1/2} = >32 min). Generally, normal diamides such as compounds (**3–22**) had exceptional HLM stability (t_{1/2} = >100 min) while reversed diamides **24–27** were poor to moderately stable (t_{1/2} = 2–32 min).

Compound **21** had the best balance of good potency, selectivity, and pharmacokinetic profile and was chosen for evaluation. In the rabbit electrically induced carotid arterial thrombosis model (ECAT).¹⁴ As depicted by Figure 5 and **21** exhibited dose-dependent reduction in thrombosis with an EC₅₀ = 2.8 μM. At the top dose, **21**

**Figure 6.** Compound **21** ex vivo aPTT vs. PT.

prolonged ex vivo aPTT by 1.8-fold but not PT, as expected with the XIa mechanism (Fig. 6).

In conclusion, phenylalanine derived diamides have been successfully established as potent and selective FXIa inhibitors. SAR and X-ray crystallography revealed that P2 prime groups in the diamides are orientated in a slightly different manner than the phenylimidazole series. Furthermore, we were able to identify molecules with subnanomolar FXIa potency by installing hydrophobic groups in the P1' region of the template. We also discovered that substituents on the core amide bond can be reversed and maintain good FXIa potency. Ultimately, our studies led to the identification of compound **21** which demonstrated good efficacy (EC₅₀ = 2.8 μM) in the rabbit electrically induced carotid arterial thrombosis model (ECAT). Further exploration of phenylalanine derived diamides will be disclosed in due course.

Acknowledgments

The authors would like to thank the BMS Department of Discovery Synthesis and BMS Biocon Research Center for the preparation of synthetic intermediates and Dr. Steven Sheriff for depositing the coordinates and data for the complexes of FXIa with compounds **6** and **27**, respectively.

References and notes

- Schumacher, W. A.; Luetzgen, J. M.; Quan, M. L.; Seiffert, D. A. *Arterioscler. Thromb. Vasc. Biol.* **2010**, *30*, 388.
- (a) Haeuël, N. H.; Nar, H.; Priepke, H.; Ries, U.; Stassen, J. M.; Wiene J. *Med. Chem.* **2002**, *45*, 1757; (b) Ieko, M. *Curr. Opin. Investig. Drugs* **2007**, *8*, 758; (c) Van Ryn, J.; Stangier, J.; Haertter, S.; Liesenfeld, K. H.; Wiene, W.; Feuring, M. *Thromb. Haemost.* **2010**, *103*, 1116; (d) Hankey, G. J.; Eikelboom *Circulation* **2011**, *123*, 1436.
- (a) Perzborn, E.; Roehring, S.; Straub, A.; Kubitz, D.; Misselwitz, F. *Nat. Rev. Drug Discovery* **2011**, *10*, 61; (b) Straub, A.; Roehrig, S.; Hillisch, A. *Curr. Top. Med. Chem.* **2010**, *10*, 257; (c) Misselwitz, F.; Berkowitz, S. D.; Perzborn, E. *Ann. N. Y. Acad. Sci.* **2011**, *1222*, 64; (d) Lassen, M. R.; Ageno, W.; Borris, L. C.; Lieberman, J. R.; Rosencher, N.; Bandel, T. J.; Misselwitz, F.; Turpie, A. G. G. *N. Engl. J. Med.* **2008**, *358*, 2776.
- (a) Pinto, D. J. P.; Orwat, M. J.; Koch, S.; Rossi, K. A.; Alexander, R. S.; Smallwood, A.; Wong, P. C.; Rendina, A. R.; Luettgen, J. M.; Knabb, R. M.; He, K.; Xin, B.; Wexler, R. R.; Lam, P. Y. S. *J. Med. Chem.* **2007**, *50*, 5339; (b) He, K.; Luettgen, J. M.; Zhang, D.; He, B.; Grace, J. E., Jr.; Xin, B.; Pinto, D. J. P.; Wong, P. C.; Knabb, R. M.; Lam, P. Y. S.; Wexler, R. R.; Grossman, S. J. *Eur. J. Drug Metab. Pharm.* **2011**, *36*, 129; (c) Pinto, D. J. P.; Smallheer, J. M.; Cheney, D. L.; Knabb, R. M.; Wexler, R. R. *J. Med. Chem.* **2010**, *53*, 6243; (d) Pinto, D. J. P.; Qiao, J. X.; Knabb, R. M. *Expert Opin. Ther. Patents* **2012**, *22*, 645.
- Furugohri, T.; Isobe, K.; Honda, Y.; Kamisato-Matsumoto, C.; Sugiyama, N.; Nagahara, T.; Morishima, Y.; Shibano, T. *J. Thromb. Haemost.* **2008**, *6*, 1542.
- (a) Hyers, T. M. *Arch. Intern. Med.* **2003**, *163*, 759; (b) Stein, P. D.; Grandison, D.; Hua, T. A. *Postgrad. Med. J.* **1994**, *70*, S72; (c) Hirsh, J.; Poller, L. *Arch. Intern. Med.* **1994**, *154*, 282.
- (a) Seligsohn, U. *J. Thromb. Haemost.* **2009**, *7*, 84; (b) Renné, T.; Oschatz, C.; Seifert, S.; Müller, F.; Antovic, J.; Karlman, M.; Benz, P. M. *J. Thromb. Haemost.* **2009**, *7*, 79.
- (a) Salomon, O.; Steinberg, D. M.; Koren-Morag, N.; Tanne, D.; Seligsohn, U. *Blood* **2008**, *111*, 4113; (b) Salomon, O.; Steinberg, D. M.; Dardik, R.; Rosenberg,

- N.; Zivelin, A.; Tamarin, I.; Ravid, B.; Berliner, S.; Seligsohn, U. *J. Thromb. Haemost.* **2003**, *1*, 658.
9. (a) Wong, P. C.; Crain, E. J.; Watson, C. A.; Schumacher, W. A. *J. Thromb. Thrombolysis* **2011**, *32*, 129; (b) Wong, P. C.; Quan, M. L.; Watson, C. A.; Crain, E. J.; Harpel, M. R.; Rendina, A. R.; Luettgen, J. M.; Wexler, R. R.; Schumacher, W. A.; Seiffert, D. A. *J. Thromb. Thrombolysis* **2015**. Ahead of Print; (c) Quan, M.; Wong, P. C.; Wang, C.; Woerner, F.; Smallheer, J. M.; Barbera, F. A.; Bozarth, J. M.; Brown, R. L.; Harpel, M. R.; Luettgen, J. M.; Morin, P. E.; Peterson, T.; Ramamurthy, V.; Rendina, A. R.; Rossi, K. A.; Watson, C. A.; Wei, A.; Zhang, G.; Seiffert, D.; Wexler, R. R. *J. Med. Chem.* **2014**, *57*, 955.
10. Büller, H. R.; Bethune, C.; Bhanot, S.; Gailani, D.; Monia, B. P.; Raskob, G. E.; Segers, A.; Verhamme, P.; Weitz, J. I. *N. Engl. J. Med.* **2015**, *372*, 232.
11. (a) Hangeland, J. J.; Friends, T. J.; Rossi, K. A.; Smallheer, J. M.; Wang, C.; Sun, Z.; Corte, J. R.; Fang, T.; Wong, P. C.; Rendina, A. R.; Barbera, F. A.; Bozarth, J. M.; Luettgen, J. M.; Watson, C. A.; Zhang, G.; Wei, A.; Ramamurthy, V.; Morin, P. E.; Bisacchi, G. S.; Subramaniam, S.; Arunachalam, P.; Mathur, A.; Seiffert, D. A.; Wexler, R. R.; Quan, M. L. *J. Med. Chem.* **2014**, *57*, 9915; (b) Hu, Z.; Wong, P. C.; Gilligan, P. J.; Han, W.; Pabbisetty, K. B.; Bozarth, J. M.; Crain, E. J.; Harper, T.; Luettgen, J. M.; Myers, J. E., Jr.; Ramamurthy, V.; Rossi, K. A.; Sheriff, S.; Watson, C. A.; Wei, Z.; Zheng, J. J.; Seiffert, D. A.; Wexler, R. R.; Quan, M. L. *ACS Med. Chem. Lett.* **2015**, *6*, 590; (c) Pinto, D. J. P.; Smallheer, J. M.; Corte, J. R.; Austin, E. J. D.; Wang, C.; Fang, T.; Smith, L. M., II; Rossi, K. A.; Rendina, A. R.; Bozarth, J. M.; Zhang, G.; Wei, A.; Ramamurthy, V.; Sheriff, S.; Myers, J. E., Jr.; Morin, P. E.; Luettgen, J. M.; Seiffert, D. A.; Quan, M. L.; Wexler, R. R. *Bioorg. Med. Chem. Lett.* **2015**, *25*, 1635.
12. Coordinates and structure amplitudes for the compound **6** (PDB ID 5E2O) and compound **27** (PDB ID 5E2P), complexes were deposited into the Protein Data Bank.
13. (a) Young, M. B.; Barrow, J. C.; Glass, K. L.; Lundell, G. F.; Newton, C. L.; Pellicore, J. M.; Rittle, K. E.; Selnick, H. G.; Stauffer, K. J.; Vacca, J. P.; Williams, P. D.; Bohn, D.; Clayton, F. C.; Cook, J. J.; Krueger, J. A.; Kuo, L. C.; Lewis, S. D.; Lucas, B. J.; McMasters, D. R.; Miller-Stein, C.; Pietrak, B. L.; Wallace, A. A.; White, R. B.; Wong, B.; Yan, Y.; Nantermet, P. G. *J. Med. Chem.* **2004**, *47*, 2995; (b) Howard, N.; Abell, C.; Blakemore, W.; Chessari, G.; Congreve, M.; Howard, S.; Jhoti, H.; Murray, C. W.; Seavers, L. C. A.; van Montfort, R. L. M. *J. Med. Chem.* **2006**, *49*, 1346.
14. Wong, P. C.; Crain, E. J.; Knabb, R. M.; Meade, R. P.; Quan, M. L.; Watson, C. A.; Wexler, R. R.; Wright, M. R.; Slee, A. M. *J. Pharmacol. Exp. Ther.* **2000**, *295*, 212.